20th Australasian Fluid Mechanics Conference
Perth, Australia
5-8 December 2016

Wake Structure of Airfoil with Serrated Trailing Edge

M. Awasthi[1], C.J. Doolan[1] and D.J. Moreau[1]

[1]School of Mechanical and Manufacturing Engineering, UNSW Australia, Sydney, 2052, Australia

Abstract

This work presents a detailed wake survey of a NACA 0012 airfoil with sawtooth type trailing edge serrations. Two different serrations with wavelengths of 0.035 and 0.052 chord lengths and each with an amplitude of 0.16 chord length were considered. The measurements were performed in an open-jet facility at a chord based Reynolds number of approximately 308,000. For each configuration, five different geometric angles of attack between 0° and 15° were also considered. The wake profiles were measured between 1% and 150% chord lengths downstream of the serrated and straight trailing edge. Results show that addition of serrations on the airfoil leads to a lower velocity deficit along the serration root possibly due to enhanced turbulent mixing and three-dimensional flow near the serrations. At lifting conditions, the serrated wake, compared to the un-serrated airfoil, shows less deflection towards the pressure side of the airfoil. Lastly, the near and far-wake structure are shown to be nearly independent of the serration wavelength.

Introduction

The trailing edge noise problem has gained much attention recently due to myriad applications ranging from airframe to wind turbine noise. While several attempts which include both active and passive devices have been made to tackle this problem, it appears that addition of trailing edge (te) extensions such as serrations is the most widely employed method. Despite of their widespread use however, little is known about the mechanism through which serrations reduce the noise. The present work is part of an ongoing attempt to understand the flow physics of serrated te's in order to develop efficient devices to aid noise reduction efforts.

One of the earliest work on serrations was a theoretical study by Howe [1] who proposed that the use of sawtooth serrations can attenuate the te noise at frequencies greater than those associated with length scales smaller than the amplitude of the serrations. This theory however assumes that the turbulence is *frozen* and the serrations reduce noise through a reduction in the scattering efficiency of the te. However, recent works such ([2], [3]) have found that the serrations lead to a noise attenuation at lower frequencies and can increase the high frequency noise. It has also been found that the serrations can supress vortex shedding noise through a reduction in the strength of the te vortex shedding [4]. These results suggest that, in addition to the scattering efficiency, the modification of the near-field hydrodynamic sources by the serrations must play a role in noise suppression mechanism. Therefore, an investigation of the effect of serrations on the flow field is desired to establish the sound source mechanism involved in these flows. Additionally, serrations are often employed in situations (e.g. wind turbine farm) where their wake can influence the overall performance of an engineering system. Therefore, it is also necessary to consider the impact of serrated te's on the far-wake flow structure.

The present work is an attempt to quantify the wake structure of sawtooth type serrations in order to understand their impact on both the near and far-wake structure through detailed measurements of the mean velocity field.

Experimental Setup

UNSW Anechoic Wind Tunnel

The measurements were performed in UNSW's Anechoic Wind Tunnel (UAT). The facility is an open-jet type wind tunnel (figure 1) where a 3m x 3.2m x 2.15m anechoic chamber is sandwiched between the contraction and diffuser sections. An axial fan located downstream of the test-section outlet provides the pressure drop within the anechoic chamber. The flow at the inlet of the facility passes through turbulence reduction screens to a contraction and is then exhausted into the test-section through a 455 mm x 455 mm square inlet (see bottom right of figure 1). The reference flow velocity during the measurements is measured at the test-section entrance using a pitot-static tube.

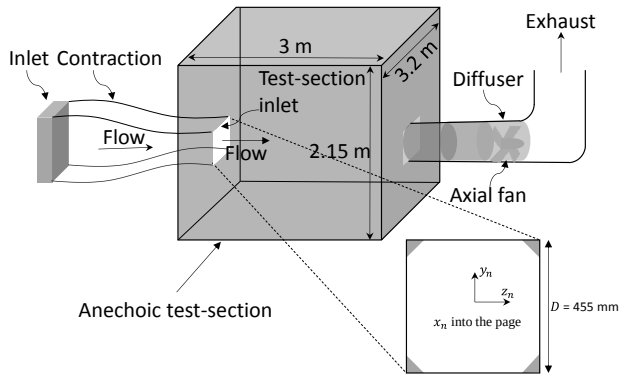

Figure 1. Schematic of UAT. Also shown at the bottom right is a zoomed in view of the test-section inlet and the tunnel-fixed coordinate system.

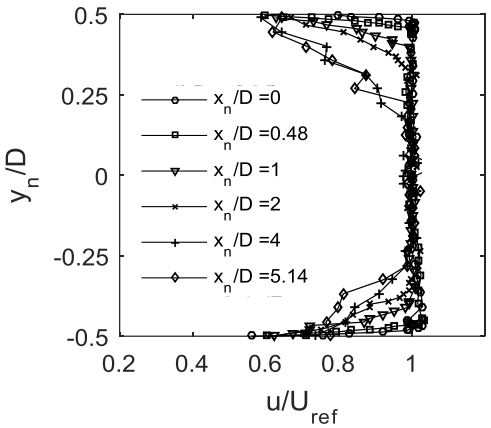

Figure 2. Streamwise variation of the UAT potential core

Figure 2 shows the streamwise variation of the jet potential-core as measured using a pitot-static tube. Here y_n, D, u, and U_{ref} refer to the vertical dimension, inlet height, local streamwise flow

velocity, and the streamwise velocity at the test-section entrance respectively. As seen in the figure, the potential jet core is stable until at least 2 nozzle diameters downstream of the nozzle exit past which it begins to deteriorate. All measurements in the present work were performed in the region with $x_n < D$.

Airfoil and Serrated Trailing Edges

The baseline airfoil used in the present work is a NACA 0012 airfoil with a chord (c) of 190 mm and a span of 455 mm. The trailing edge (te) of the airfoil is blunt and rounded with a diameter of 3 mm. To install the serrations a 16 x 1.5 mm slit was created at the te Figure 3a shows the airfoil profile along with the slit location at the te. This slit was used to add te serrations as well as a flat plate to compare the un-serrated and serrated te response to the flow. Figure 3b shows a top-view schematic of the reference and the two types of serrations considered in the present work. Each of the three configurations shown in figure 3b have a streamwise length of 38 mm bringing the overall chord of the airfoil to 228 mm. Both serrations are sawtooth type serrations with two different wavelengths (λ) of 8 mm and 12 mm. The airfoil was mounted in the test-section by installing two end-plates and bolting the airfoil to them (figure 3c). The leading edge of the airfoil (at zero angle of attack) was located 30 mm downstream of the inlet exit plane. The angle of attack of the airfoil was changed by rotating it about baseline airfoil's mid-chord as shown in figure 3a. Five different geometric angles of attack (α_g) equal to 0, 5, 10, 12, and 15 degrees were considered in the present work. Figure 4c also shows the coordinate system definition which will be followed throughout the presentation of results. The origin of the coordinate system is at the te (serrated or otherwise) of the airfoil. The coordinate system is flow-fixed i.e. x and y coordinates are parallel and perpendicular to the flow direction respectively. The spanwise coordinate z completes the right hand rule.

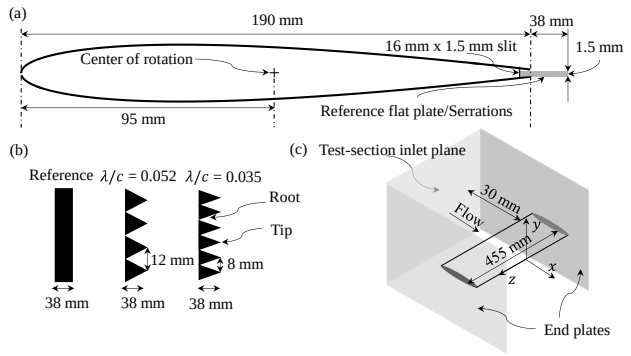

Figure 3. Schematic of test configurations. (a) NACA0012 airfoil profile with serrated/un-serrated te extension. (b) Reference and serrated te geometry. (c) Airfoil setup in UAT test-section along with the coordinate system definition.

Instrumentation and Measurement Uncertainties

The flow velocity in the test-section was measured at the inlet exit plane using a pitot-static tube. The stagnation and static pressure from the tube were measured using a Scanivalve® DSA 2317 pressure scanner which has a range of 2488.4 Pa and an uncertainty of $\pm$4.97 Pa. A Vaisala® PTU300 unit was used to monitor the ambient pressure and temperature with uncertainties of $\pm$10 Pa and $\pm$0.2°C respectively. The wake velocity profiles were measured using a flattened pitot probe mounted on a three-dimensional Dantec Dynamic® traverse system which has a positional uncertainty of 6.25 μm. The external and internal diameter of the pitot probe were 1.25 mm and 0.75 mm respectively. The static pressure in the anechoic chamber was measured using a plastic tube near the inlet exit plane. The uncertainty in mean velocity obtained by combining the aforementioned uncertainties is $\pm$0.25 m/s. For the baseline and reference airfoils the profiles were measured at the mid-span while for the serrated te's they were measured at the root of each serration. The streamwise locations at which profiles were measured are x/c = 0.01, 0.02, 0.05, 0.1, 0.2, 0.3, 0.4, and 0.5. Note that x = 0 is defined at the te of the airfoil.

Aerodynamic Corrections

The finite size of an open-jet flow over an airfoil results in flow curvature which would not exist in a free-flight. This curvature results in a lower free-flight angle of attack (α_f) corresponding to a particular α_g in an open-jet flow. The α_f for the present work were calculated using the method developed by [5] and are reported in table 1.

α_g	0	5	10	12	15
α_f	0	2.7	5.4	6.4	8

Table 1. Free-flight angles of attack corresponding to the geometric angles in the present work.

It is well known that the presence of airfoil in wind tunnels leads to blockage effect (see [6] for example) which results in a lower local free-stream velocity (U_e) behind the airfoil. There are two components to this blockage, namely solid and wake blockage, both of which increase with increasing angles of attack. Figure 4a which shows the wake profiles at x/c = 0.01 for the reference case provides an illustration of the blockage effect. These profiles have been normalized on the velocity U_{ref} measured upstream of the airfoil. It can be seen that though each profile approaches an asymptotic value, this value for higher angles of attack (α_g> 5°) is lower than 1. This is due to an increase in the solid blockage and a larger wake for higher angles of attack which results in a lower U_e. Therefore, in the discussion hereafter each profile has been normalized on the local free-stream velocity (U_e) rather than U_{ref} as shown in figure 3b.

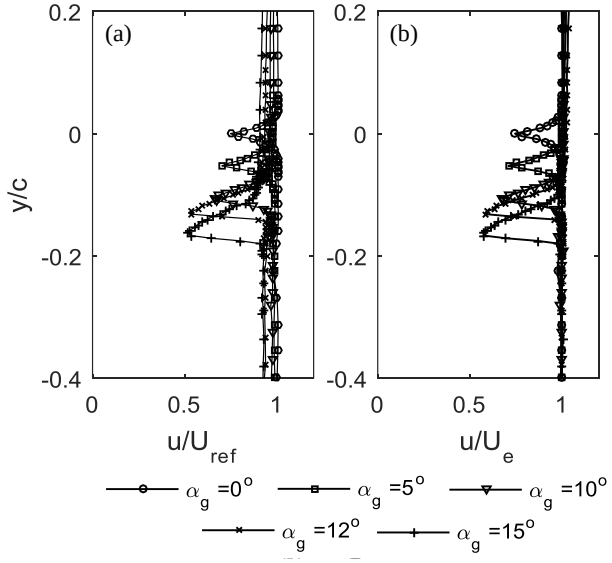

Figure 4. Illustration of solid and wake blockage correction of free-stream velocity through wake profiles at x/c = 0.01 for Reference airfoil. (a) Wake-velocity normalized on U_{ref} and (b) Wake-velocity normalized on U_e.

Results and Discussion

Wake Structure of Baseline and Reference Airfoil

Before we present the results for serrated te's it is worthwhile to consider the differences between the wake structure of the baseline NACA0012 airfoil and the reference airfoil with the flat-plate attached to the te. Figure 4 shows the wake profiles at three

measurement stations downstream of the two airfoils at α_g = 0°. In the near wake (x/c = 0.01) the overall wake structure for the two cases is similar except that the baseline case shows a broader wake and a lower velocity deficit. This is because the te of the baseline case is thicker and is rounded. Further downstream at x/c = 0.1, the baseline airfoil wake is still thicker but the velocity deficit is less than that seen upstream. In the far-wake (x/c = 0.5) the two profiles look quite similar in magnitude but the lingering effects of the thicker baseline airfoil te are still apparent.

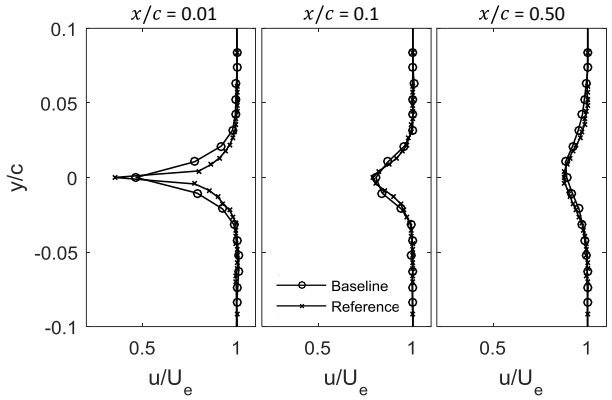

Figure5. Wake structure of baseline NACA0012 and reference airfoil at α_g = 0°

Wake Structure of Serrated Trailing Edges

Let us now consider the effect of serrated te's on near and far-wake profiles. Figure 6 shows the wake profiles of the two serrated te's along with the reference case for α_g = 0° at three streamwise stations. In the near-wake (x/c = 0.01) the wake profile for serrated te's has the same shape as the reference airfoil but shows a lower velocity deficit (weaker wake) than the latter. The presence of serrations, however, do not alter the location of the dip in the wake profile. The change in wake intensity is likely due to the flow separation which occurs further upstream in the serrated case and leads to locally three-dimensional flow in the near-wake. A similar weakening of wake along the serration root has also been observed previously by Liu *et al.* [7]. As we move further downstream to x/c = 0.1 the difference between the serrated and reference airfoil wake strength is reduced but the effect of serrations can clearly be observed. In the far-wake (x/c = 0.5) each case has almost similar wake profile but the serrated wake still appears to be slightly weaker showing that the effect of flow structure alteration by serrations can affect the flow far downstream. Another interesting observation from figure 6 is that changing the wavelength of sawtooth serration appears to have negligible influence on the wake structure, even in close proximity to the te.

While at zero lift condition the serrations seem to only affect the wake strength, it is beneficial to consider their effect on lifting airfoil since in practice serrations are employed to reduce noise from high lift devices. To better visualize multiple angles of attack and measurement locations, figure 7 shows contours of wake-velocity for the three configurations and five angles of attack considered in the present work. The contour levels between the actual measurement locations (shown as vertical dashed lines on each plot) were obtained using linear interpolation. Each plot also shows the chord line of the airfoil projected to the wake region. Considering the reference airfoil first (left column) we see a typical airfoil wake behaviour in that the wake is deflected towards the pressure side (downwards) with increasing α_g and it becomes stronger in magnitude due to thickening and eventual separation (stall) of the boundary layer on the suction side. Consider now the effect of serrated te on wake structure as shown in the middle and right column of figure 7. We first note that changing the wavelength of serrations has little impact on the overall wake structure and its intensity. Furthermore, at each angle of attack due to enhanced turbulent mixing provided by the serrations, the serrated wake is weaker than the reference case similar to what was observed at α_g= 0° in figure 6. However, the contours shown in figure 7 for lifting conditions also display a qualitative change in wake structure due to serrations. For both serrations, increasing the angle of attack causes less downward deflection of the wake compared to the reference case. This suggests that there is an overall upward flow deflection within the root region of the serrations. A similar result, but for cambered airfoil, has been previously demonstrated by Liu *et al.* [7].

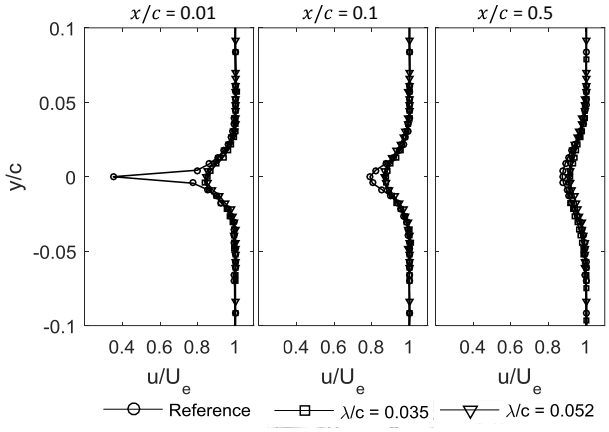

Figure 6. Effect of trailing edge serrations on wake structure at α_g = 0°.

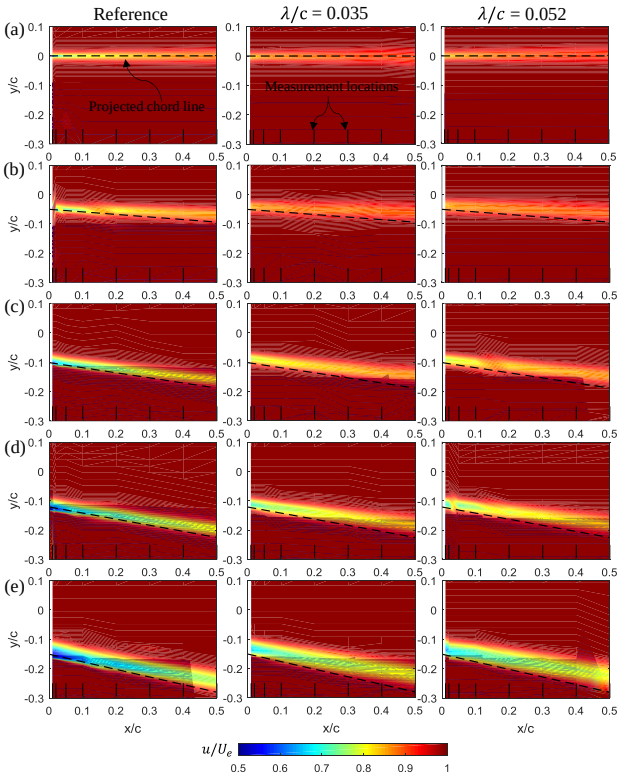

Figure 7. Wake-velocity contours for reference and serrated airfoil at five different geometric angles of attack: (a) α_g = 0°, (b) α_g = 5°, (c) α_g = 10°, (d) α_g = 12°, and (e) α_g = 15°.

To further investigate the impact of serrations on wake structure consider figure 8a which shows the location of minimum wake velocity ($y_{u,min}$) as a function of angle of attack at three different streamwise locations. We first note that that for each of the cases shown here $y_{u,min}$ varies almost linearly with α_g. At α_g = 0° the

minimum wake velocity for all three cases appears exactly at the base of the te For $\alpha_g \neq 0°$ $y_{u,min}$ appears to be independent of λ and shifts towards the suction side compared to the reference case as the angle of attack is increased. Figure 8b shows the variation of minimum wake-velocity (wake-strength) as a function of streamwise distance for all three configurations and three different α_g. For the reference case the velocity deficit at α_g = 0° is higher compared to α_g > 0 near the te but rises more rapidly to an asymptotic value as the distance from te increases. The wake-strength for the two serrations is identical even in the near-wake region and compared to the reference case both display a weaker wake at each value of α_g.

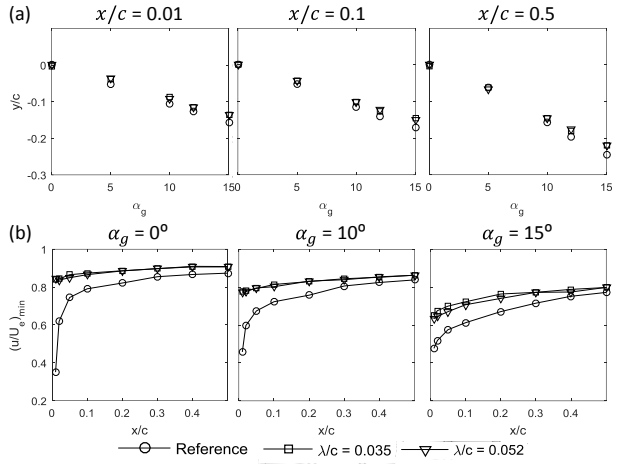

Figure 8. (a) Minimum wake-velocity locations as a function of angle of attack and (b) Minimum wake-velocity as a function of streamwise distance for three angles of attack.

Conclusions

Measurements of mean velocity in the wake of a NACA 0012 airfoil with and without sawtooth type serrations were performed in an open-jet facility. The chord based Reynolds number in the experiments was approximately 308,000 and measurements were performed for five different geometric angles of attack between 0° and 15°. The results show that the presence of serrations leads to a lower velocity deficit along the root of the serrations in both the near and far-wake. The presence of serrations also modifies the wake structure at non-zero angles of attack in that the minimum wake-velocity location shifts towards the suction side. The wavelength of the serrations however have negligible quantitative or qualitative influence on the wake structure in both near and far-wake regions.

References

[1] Howe, M.S., Noise produced by a sawtooth trailing edge," Journal of the Acoustical Society of America, Vol. 90, 1991, pp. 482-487.

[2] Oerlemans, S., Fisher, M., Maeder, T., and Kogler, K., "Reduction of wind turbine noise using optimized airfoils and trailing-edge serrations," AIAA Journal, Vol. 47(6), 2009, pp.1470-1481.

[3] Gruber, M., Joseph, P., and Chong, T., "Experimental investigation of airfoil self-noise and turbulent wake reduction by the use of trailing edge serrations," 16th AIAA/CEAS Aeroacoustics Conference, Stockholm, Sweden, 7 - 9 June 2010.

[4] Moreau D.J., Brooks L.A., and Doolan C.J., (2013), "On the Noise Reduction Mechanism of a Flat Plate Serrated Trailing Edge at Low-to-Moderate Reynolds Number." AIAA 51(10): 2513-2522.

[5] Maskell, E.C., "A theory of blockage effect on bluff bodies and stalled wings in a closer wind tunnel," ARC R&M 3400, 1963.

[6] Brooks, T.F., Marcollini, M.A, Pope, D.S., "Airfoil trailing edge flow measurements ," AIAA Journal, Vol. 24 (8), 1986, pp. 1245-1251.

[7] Liu, X., Jawahar, H.K., Azarpeywand, M., "Wake Development of Airfoils with Serrated Trailing Edges," 22nd AIAA Aeroacoustics Conference, Lyon, France, 30 May – 1 June 2016.